Dual-Phase DC-DC Converter for Fuel Cell Power Supply in Transportation

Haiping Xu, Ermin Qiao, Xin Guo, Xuhui Wen, Li Kong
Institute of Electrical Engineering, Chinese Academy of Sciences
Beijing, P.R.China, 100080
Phone: 86-10-62583864, E-mail: hpxu@mail.iee.ac.cn

Keywords: DC-DC Converter, Fuel Cell, Electric Vehicle

Abstract: This article proposes a topology of high power Dual-Phase Boost DC-DC Converter for Fuel Cell Power Supply. The operating principle of the converter operating in CCM (continuous conducting mode) is analyzed thoroughly. The State-Space-Averaged Model of the system is developed. Based on the small signal transfer function the two-loop controllers were designed, and a 150 kW Converter is constructed. The experimental results show that the efficiency of the converter is over 97%. It can be applied in the EV as well as the distributed power station and energy storage system.

1 Introduction

Fuel Cell Electric Vehicle (FCEV) is believed to be the ultimate target in the development of EV in 21st century. In the FCEV, High power DC-DC converter is adopted to adjust the output voltage, current and power of Fuel Cell Engine (FCE) to meet the vehicle's requirements. As Fig.1 shows, the power supply system of FCEV is composed of Proton Exchange Membrane Fuel Cell (PEMFC), high power DC-DC converter, Battery (B), and Bi-directional DC-DC converter.

In the application of FCEV and moveable Power Supply, the power converter devices especially demand small volume, light weight, stable and reliable properties, that is to say, DC-DC converter need high power density and excellent dynamic control characteristic. Boost converter has such good properties, simple system structure, high conversion efficiency and good stability and reliability, that it can be widely applied in EV. In the high power Boost converter, a high power magnetic inductor is the important unit, which mainly composes the whole volume and weight of the device. It is a very hard and challenging work to design a high power inductor to store energy.

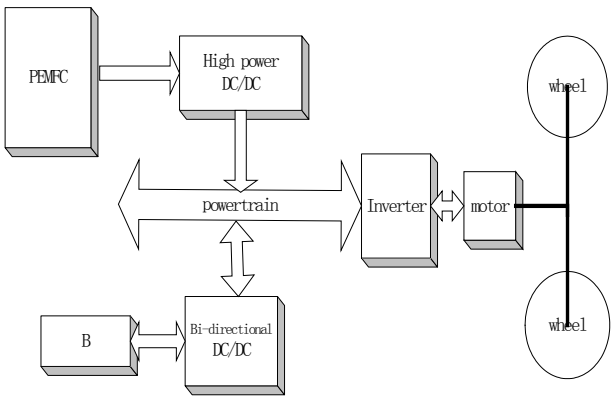

Fig 1. The power supply system of FCEV

In this paper, a Dual-Phase Boost DC-DC converter [2][3] is presented, that greatly decreases the volume and weight of the converter and improves reliability of the system.

2 The principle of Dual-Phase DC-DC Converter

The Dual-Phase DC-DC Converter is shown in Fig 2. The principle of Dual-Phase Boost DC-DC Converter as follows: each phase is a Boost/Buck DC-DC Converter, which is composed of a bridge of power switches and storage energy inductor. When S1u=S2u=OFF, S1d and S2d switch on and off,

the system work in the Boost mode, and the power switches S1d and S2d have 180-degree phase difference of driving pulses in a cycle. The fluctuation of input power supply is reduced greatly because the two 180-degree phase difference inductor currents minify the fluctuation of each other [1] [4]. So, in the process of the system design, under the same current fluctuation coefficient condition, inductor L1 and L2 can be adopted less inductance value and half current rating correspondingly.

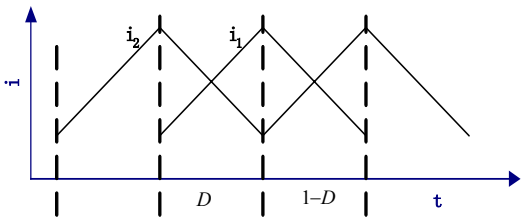

Fig 3. The current waveforms of the two inductors

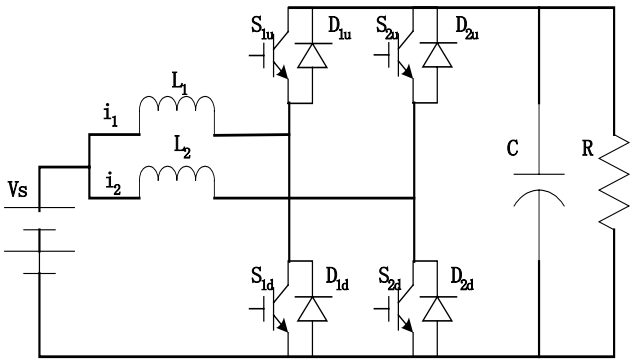

Fig 2. The topology of the DC-DC converter

The current waveforms of two-phase inductors are showed in Fig 3. As Fig.3 shows, in one switching cycle T, the converter have two kinds of running state at corresponding period, the sub-circuits are as follows:

1) 0<t<D*T：The power switch S1d and anti-paralleled diode D2u are conducting and the equivalent sub-circuit 1 is show in fig 4a,

2) D*T<t<T：The power switch S2d and anti-paralleled diode D1u are conducting and the equivalent sub-circuit 2 is show in fig 4b.

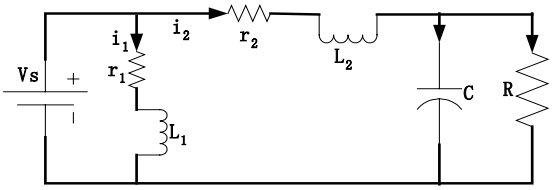

Fig 4a. The equivalent sub-circuit 1

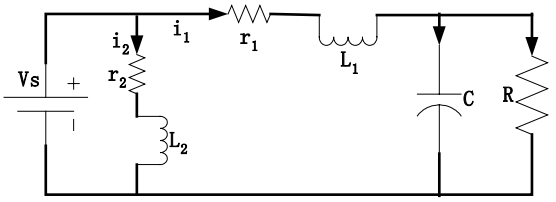

Fig 4b. The equivalent sub-circuit 2

3 State-Space Averaged System Model

The modeling and analysis of the system is carried under the following: 1) power switches of the converter are assumed to be ideal, 2) The equivalent series resistance of the capacitance is neglected, 3) The two parallel boost cells operate in the continuous inductor current mode (CCM) and the two switches (S1d, S2d) operate in the interleaved fashion.

The state space equations are separately established according to the equivalent circuits in Fig 4. Supposing i_1, i_2, V_c as the state variables and V_s as the variable of the input voltage and V_0 as the variable of the output voltage,

State space equation of equivalent sub-circuit 1 as fig 4a:

$$\dot{X} = A_1 X + B_1 V_S \ldots\ldots during..D*T_s \qquad A_1 = \begin{bmatrix} -\frac{r_1}{L_1} & 0 & 0 \\ 0 & -\frac{r_2}{L_2} & -\frac{1}{L_2} \\ 0 & \frac{1}{C} & -\frac{1}{RC} \end{bmatrix}, B_1 = \begin{bmatrix} \frac{1}{L_1} \\ \frac{1}{L_2} \\ 0 \end{bmatrix}, C_1 = \begin{bmatrix} 0 & 0 & 1 \end{bmatrix}$$

$$V_0 = C_1 X$$

State space equation of equivalent sub-circuit 2 as fig 4b:

$$\dot{X} = A_2 X + B_2 V_S ....during..(1-D)*T_s \qquad A_2 = \begin{bmatrix} -\frac{r_1}{L_1} & 0 & -\frac{1}{L_1} \\ 0 & -\frac{r_2}{L_2} & 0 \\ \frac{1}{C} & 0 & -\frac{1}{RC} \end{bmatrix}, B_2 = \begin{bmatrix} \frac{1}{L_1} \\ \frac{1}{L_2} \\ 0 \end{bmatrix}, C_2 = \begin{bmatrix} 0 & 0 & 1 \end{bmatrix}$$
$$V_0 = C_2 X$$

AVERAGING: the state-spaced equations of two sub-circuit modes are time weighted and averaged over the switching period T_s .

$$\dot{X} = (A_1 * D + A_2 * (1-D))X + (B_1 * D + B_2 * (1-D))V_S \quad \text{.....(1)}$$
$$V_0 = (C_1 * D + C_2 * (1-D))X$$

The state matrix A，B and C are：

$$A = \begin{bmatrix} -\frac{r_1}{L_1} & 0 & -\frac{(1-D)}{L_1} \\ 0 & -\frac{r_2}{L_2} & -\frac{D}{L_2} \\ \frac{(1-D)}{C} & \frac{D}{C} & -\frac{1}{RC} \end{bmatrix}, \ldots B = \begin{bmatrix} \frac{1}{L_1} \\ \frac{1}{L_2} \\ 0 \end{bmatrix}, \ldots C = \begin{bmatrix} 0 & 0 & 1 \end{bmatrix} \quad \text{……. (2)}$$

On the assumption that the two phase circuits is symmetrical, so, $L_1 = L_2$, $r_1 = r_2$.

$$X = -A^{-1}BV_s$$
$$V_0 = -CA^{-1}BV_S \quad \text{…… ...…….(3)}$$

The static characteristics of the converter are:

$$M = \frac{V_0}{V_s} = \frac{1}{1-D}$$
$$I_1 = I_2 = \frac{V_S}{2R(1-D)^2} \quad \text{……..… (4)}$$
$$V_0 = \frac{V_S}{1-D}$$

4 The Design of the Controller

A. System transfer function

Considering the effect of the control variable D, the state-space averaged equation is described to,

$$\dot{X} = F(x, v_s, d) \text{ ,} \quad \text{……(5)}$$

The small signal model of the converter is:

$$\dot{\hat{x}} = A'\hat{x} + B'\hat{v}_s + K\hat{d} \quad \text{……..…….(6)}$$
$$A' = \frac{\partial F}{\partial x}, B' = \frac{\partial F}{\partial v_s}, K = \frac{\partial F}{\partial d}$$

The control to state variable transfer functions is:

$$\frac{\hat{x}}{\hat{d}} = (sI - A')^{-1} K \quad \text{……..……(7)}$$

G_{id} : Open loop control to inductor current transfer function,

$$Gid(s) = \frac{RCV_0 * s + 2V_0}{RLC * s^2 + L * s + R(1-D)^2} \quad \text{……..…(8)}$$

G_{vd} : Open loop control to output voltage transfer function,

$$Gvd(s) = \frac{-LV_0/(1-D) * s + V_0 R(1-D)}{RLC * s^2 + L * s + R(1-D)^2} \quad \text{…….(9)}$$

B. Design of Digital Controller

Based on the transfer function above, the BODE PLOT can be drawn and the digital controller can be designed. The control system of this converter is a double closed-loop, outer voltage loop and inner current loop, fully digitalized with DSP, The dual-loop controller is shown in Fig 5.

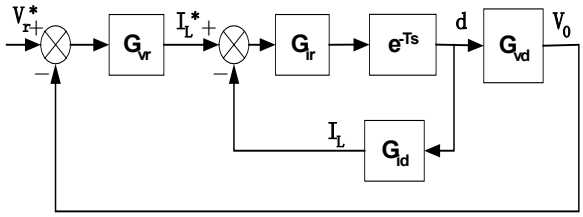

Fig 5. The dual-loop controller of the converter

The loop gains for inner current loop and outer voltage loop can be expressed as:

$$H_i(s) = G_{ir} * G_{id} * e^{-Ts} \quad \text{……..…… (10)}$$

$$H_v(s) = \frac{G_{vr} * G_{ir} * e^{-Ts} * G_{vd}}{1 + H_i} \quad \text{……..…(11)}$$

H_i : Current loop gain, H_v : voltage loop gain,

G_{ir} : Current loop Compensator, G_{vr} : Voltage loop Compensator

e^{-Ts} : Delay caused by sampling period, computation time and duty cycle update,

Design of the Boost Current Compensator: To devise the Compensator the Matlab program is designed. The program allows compensators to be designed graphically by placing poles and zeros and then adjusting the gain for the desired crossover and phase margin. The program continually computes the open loop response; shows the gain and phase margin, and then determine stability of the system. The transfer function of the current compensator is:

$$Gir(s) = 6 * \frac{s/180 + 1}{s(s/2000 + 1)}$$

Design of the Boost Voltage Compensator: With the current compensator designed, the voltage compensator can be designed by looking at the response of $H_2 = \frac{H_v}{1+H_i}$. The same procedure was used to import the control-to-output transfer function and the associated sensor gain and filter dynamics. The transfer function of the voltage compensator is:

$$Gvr(s) = 12 * \frac{s/12 + 1}{s(s/10000 + 1)}$$

5 Experimental Result

Based on the analysis above, a prototype of a fully digitalized Dual-Phase Boost converter was constructed with its basic technical specification as follows: P=150 kW, 250 V $\leq V_s \leq$450V, V_0 =584 V. The proposed converter weigh 50Kg and hold 50L，which lessen one-third of the volume and weight than single phase Boost converter, moreover, the fluctuation of current is less than 10 %.

Figures.6 are the waveforms of the Dual-Phase Boost converter working at 75kW. Fig 6a are the waveforms of its output voltage and current, which shows that the voltage and current fluctuation is less than 1%. Fig 6b are the waveforms of the Inductor current of one phase and output voltage. Fig 6c are the waveforms of two phases Inductor current at half load. Fig 7 are the waveforms of output voltage and current when the system is soft started and stopped. From the waveforms we can see that the soft start period is 2s. Fig 8 is the system efficiency curve, which indicates that the whole efficiency is about 95~98%，and the efficiency is over 97% when the output power is large than the half of rated power .

The related parameters of the oscillograph are: voltage—200V/div, current—100A/div.

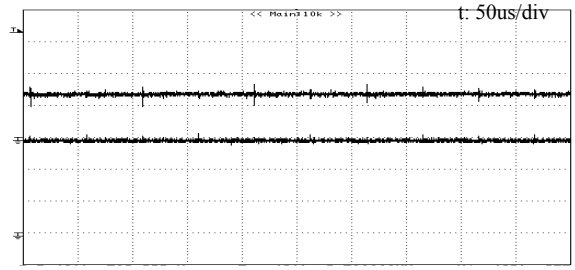

Fig 6a：Output current (upper) and output voltage (lower)

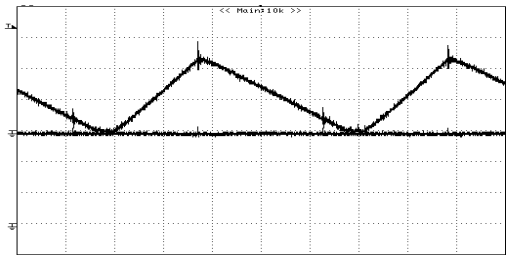

Fig 6b：Inductor current (upper) and output voltage (lower)

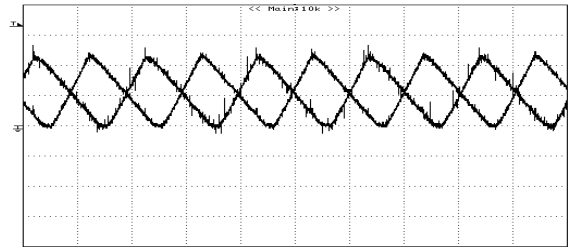

Fig 6c：Two phase Inductor current

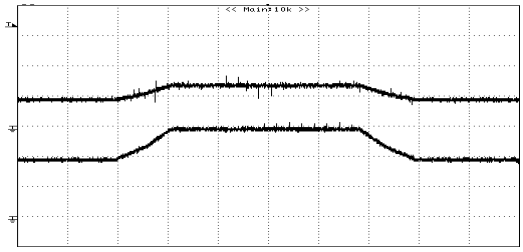

Fig 7：Output current (upper) and voltage (lower) at soft start/stop

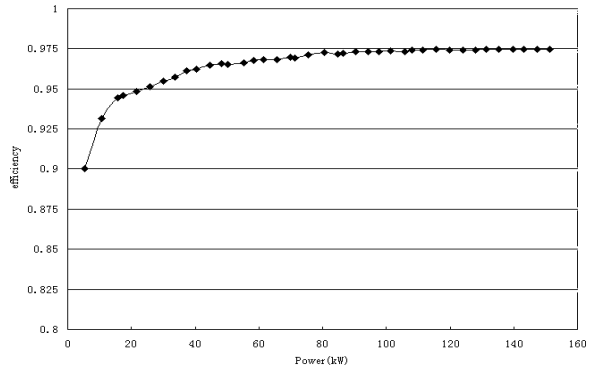

Fig 8：The system efficiency curve

6 Conclusions

In conclusion, the efficiency of the Dual-Phase Boost DC-DC Converter is over 97%, and the volume and weight is decreased one-third than conventional Boost converter. Owing to the digital control its dynamic characteristic is excellent. Therefore, the proposed Dual-Phase Boost converter is suitable for Fuel Cell Electric Vehicle as well as the Fuel Cell Distributed Generation.

References

[1] David J. Perreault and Jhon G.Kassakian . “Distributed interleaving of paralleled power converters”. IEEE Trans. on Power Electronics, Vol. 9(4), pp.405-413, 1994

[2] Xudong Huang, Nergaard. T, Jih-Sheng Lai, Xingyi Xu, Lizhi Zhu. “A DSP based controller for high-power interleaved boost converters”. APEC '03, 9-13 Feb. 2003, Pages: 327 - 333 vol.1.

[3] X. Huang, X. Wang, J. Ferrell, T. Nergaard, J. Lai, X, Xu and L.Zhu, “Parasitic Ringing and Design Issues of High Power Interleaved Boost Converters,” in Conf. Rec. of IEEE Power Electronics Specialists Conference, 2002.

[4] Zang M.T., Jovanovic, M.M., and Lee F.C. “Analysis and evaluation of interleaving techniques in forward converters”. IEEE Trans. on Power Electronics, Vol. 13(4), pp.690-697, 1998.

[5] Jai P.AgrawaL. “Power electronic systems : theory and design”. Prentice-Hall Press, 2001